



Published in final edited form as:

*Biofabrication*. 2014 June ; 6(2): 025007. doi:10.1088/1758-5082/6/2/025007.

## Generating size-controlled embryoid bodies using laser direct-write

AD Dias<sup>1</sup>, AM Unser<sup>2</sup>, Y Xie<sup>2</sup>, DB Chrisey<sup>3</sup>, and DT Corr<sup>1,\*</sup>

<sup>1</sup>Department of Biomedical Engineering, Rensselaer Polytechnic Institute, 110 Eighth Street, Troy, NY 12180, USA

<sup>2</sup>College of Nanoscale Science and Engineering, State University of New York, 257 Fuller Road, Albany, NY 12203, USA

<sup>3</sup>Department of Physics and Engineering Physics, Tulane University, 6823 St. Charles Avenue, New Orleans, LA 70118, USA

### Abstract

Embryonic stem cells (ESCs) have the potential to self-renew and differentiate into any specialized cell type. One common method to differentiate ESCs *in vitro* is through embryoid bodies (EBs), 3D cellular aggregates that spontaneously self-assemble and generally express markers for the three germ layers, endoderm, ectoderm, and mesoderm. It has been previously shown that both EB size and 2D colony size each influence differentiation. We hypothesized that we could control the size of the EB formed by mouse ESCs (mESCs) by using a cell printing method, laser direct-write (LDW), to control both the size of the initial printed colony and the local cell density in printed colonies. After printing mESCs at various printed colony sizes and printing densities, two-way ANOVAs indicated that EB diameter was influenced by printing density after 3 days ( $p = 0.0002$ ), while there was no effect of printed colony diameter on EB diameter at the same timepoint ( $p = 0.74$ ). There was no significant interaction between these two factors. Tukey's Honestly Significant Difference test showed that high-density colonies formed significantly larger EBs, suggesting that printed mESCs quickly aggregate with nearby cells. Thus, EBs can be engineered to a desired size by controlling printing density, which will influence the design of future differentiation studies. Herein, we highlight the capacity of LDW to control the local cell density and colony size independently, at prescribed spatial locations, potentially leading to better stem cell maintenance and directed differentiation.

### Keywords

Stem cell; cell printing; microenvironment; differentiation

---

\*Corresponding author. David T. Corr, Associate Professor, Department of Biomedical Engineering, Rensselaer Polytechnic Institute, 110 8th Street, Troy, NY 12180, Phone: (518) 276-3276, Fax: (518) 276-3035, corrd@rpi.edu.

No competing financial interests exist.

## 1. Introduction

Embryonic stem cells (ESCs) are capable of self-renewal and have the potential to differentiate into any specialized cell type [1]. If this differentiation potential can be harnessed, cell sources can be generated for therapeutic applications, including tissue regeneration and cell replacement. However, uncontrolled differentiation of ESCs typically results in the formation of teratomas or spontaneous differentiation into undesired cell types [2–4]. Therefore, understanding and directing this differentiation potential is critical to producing cell sources for tissue engineering and replacement therapies.

One method to promote ESC differentiation *in vitro* is the formation of three-dimensional cellular aggregates known as embryoid bodies (EBs), which spontaneously form via cell clustering [3,5]. These EBs share some characteristics of the developing embryo, including the presence of the three primitive germ layers, endoderm, mesoderm, and ectoderm. Additionally, EBs grown *in vitro* display many parallels to the spatiotemporal development of the post-implantation mouse embryo [6]. Although mimicking the complex spatiotemporal development of the embryo is difficult, the addition of factors such as retinoic acid (RA) can enable basic levels of organization [7]. It is well known that numerous mechanical [8,9] and soluble [10] signals, population heterogeneity [11], and coculture [12] influence differentiation and maintenance of pluripotency, but confounded with these factors are the aggregate and EB sizes.

ESC differentiation potential and efficiency is influenced by aggregate and EB sizes [13–18]. EB size is dependent on the number of cells that initially self-assemble by cell-cell adhesion [5]. Previous work using mouse ESCs (mESCs), and a micropatterning technique to control planar cell aggregate size, has shown that EB aggregates of different size exhibit different gene expression; 100- $\mu\text{m}$ -diameter aggregates expressed increased ectoderm markers while 500- $\mu\text{m}$ -diameter aggregates expressed endoderm and mesoderm markers [19]. In other studies utilizing human ESCs, large cell colonies gave rise to mesoderm, while small colonies formed endoderm [20]. Human ESC differentiation based on colony size can be rescued by a Rho-associated kinase (ROCK) inhibitor [21], suggesting that cell-cell adhesion and cytoskeletal organization are critical regulators of differentiation. These studies suggest that planar cellular aggregate size is important in EB formation and differentiation. However, a potential limitation of micropatterning is that cell growth is restricted to adhesion islands, and initial cell density on adhesion islands is not precisely controlled. Constrained cell growth restricts the total number of cells that can be generated without enzymatic treatment, and enzymatic cell dissociation removes organization from their initial configuration. Moreover, cells seeded on adhesion islands are initially locally confluent, eliminating local cell density as a differentiation parameter.

In addition to planar aggregate size, 3D EB size may also influence differentiation. When concave microwells were used to control EB size, and the retrieved EBs were cultured in neural differentiation medium, larger EBs exhibited more neurites and longer neurite outgrowths than smaller EBs [22]. When these retrieved EBs were differentiated toward the endothelial or cardiac lineage, smaller EBs showed greater angiogenic sprouting activity, while larger EBs had a higher beating frequency [22,23]. Because EB size at this timepoint

influences differentiation, stem cells can be “primed” at this early differentiation stage by controlling the EB size via the geometric microenvironment so that later directed differentiation into adult cell types is more efficient [13]. However, restricted growth in concave microwells only allows for control of the initial number of seeded cells and the type of media in the microenvironment. Removal of EBs from the microwells is required for subsequent differentiation. It may be desirable to control other aspects of the stem cell microenvironment, such as paracrine signaling from other colonies or EBs, and mechanical/materials signaling from the substrate.

The gold standard for EB formation is aggregation and growth of ESCs in “hanging drops,” where droplets of cell suspension are pipetted onto the lid of a Petri dish, and EBs form within the droplet [24]. Because all of the cells aggregate by gravity as a single mass within the droplet, EB size is determined by the initial number of cells and time allowed to proliferate. Inkjet bioprinting has been used as a high-throughput method for generating hanging drops [25,26], and the use of inverted microwells to reduce the radius of curvature of hanging drops improved EB formation with a high initial cell number [27]. Various other methods for EB generation have been utilized [28], including stirred suspension culture [29,30], hydrophobic surface treatment [31], centrifugation [32], and various types of microwells [33–35] or degradable scaffolds [36]. Stirred suspension culture in particular has attracted attention for ESC culture because of scalability of controlled-size EBs and unrestricted growth potential [28]. However, suspension culture, and other conventional methods for EB generation, do not provide suitable control over localized cell density, nor do they allow controlled interactions between EBs and between the EB and the substrate during early differentiation. In order to study whether these interactions are important, a technique to precisely place controlled-size EBs on homogeneous substrates must be established.

Various mechanisms have been proposed for the influence of EB size on differentiation, including mass transport [16,37], geometric constraints and organization [14], and cell-cell contact [38]. While EBs generally grow over time, it is desirable to control the size at a given timepoint because differentiation depends on both spatial and temporal signaling [6]. Moreover, EB formation should be consistent, because differences in EB structural morphology, such as cavity formation, influence subsequent differentiation [39].

To address the aforementioned limitations, the aim of this study was to control EB size on a homogeneous substrate with unrestricted cell growth potential via laser direct-write (LDW) cell printing (Fig. 1). Our lab has shown that mESCs printed using LDW maintain their pluripotency and are capable of forming EBs [40]. We hypothesized that we could influence EB size by using LDW to control the size of a printed mESC colony and the local cell density within the colony. To test this hypothesis, we printed patterns of mESCs at different colony sizes and cell densities within colonies and measured the size of the resultant EBs. LDW provided the necessary control over the microenvironment to perform this study.

## 2. Materials and Methods

### 2.1 Cell maintenance

CCE mESCs (StemCell Technologies, Vancouver, BC, Canada) were grown in standard ES maintenance media with 15% fetal bovine serum, 1 mM sodium pyruvate, 100 U/mL penicillin/streptomycin, 2 mM L-Glutamine, 0.1 mM MEM non-essential amino acids, 10 ng/mL leukemia inhibitory factor (LIF), and 100  $\mu$ M monothioglycerol in Dulbecco's Modification of Eagle's Medium (DMEM) high glucose [41,42]. Cells were passaged every 2–3 days with 0.1% trypsin/EDTA onto 0.1% gelatin-coated tissue culture flasks.

### 2.2 Laser direct-write and embryoid body formation

Following previously established methods, a gelatin-based LDW technique [43] was used to deposit cells on glass cover slips [44] (Fig. 1). Briefly, cover slips were etched in 90% sulfuric acid/10% hydrogen peroxide. After washing with distilled water and ethanol, cover slips were air dried, plasma cleaned, and coated with poly-L-lysine (100  $\mu$ g/mL). After air drying, cover slips were spin-coated with warm 10% gelatin/DMEM at 4000 rpm and placed on a 20% gelatin/DMEM-coated Petri dish at 4 °C. The dish/cover slip system was rinsed with cold DMEM, and 7.0  $\mu$ L of ES maintenance media were added to each cover slip shortly before cell deposition for short-term maintenance.

To prepare a “print ribbon”, a UV-transparent quartz disk (Edmund Optics, Barrington, NJ) was spin-coated with 20% gelatin/DMEM at 2000 rpm and incubated at 37 °C prior to seeding with cells. Cells were trypsinized and resuspended in media without LIF after centrifugation. A cell suspension ( $1 \times 10^6$  –  $1 \times 10^7$  cells, depending on desired density) was triturated and pipetted onto the ribbon, and the cell-loaded ribbon was incubated at 37 °C for seven minutes, then placed in a biosafety cabinet at 24 °C for five minutes.

Excess media was then removed from the ribbon, and the ribbon was placed in the path of a laser objective. Petri dishes containing prepared glass coverslips were placed underneath the ribbon such that cells on the ribbon were 600  $\mu$ m from the cover slip surface. To “print” cells, a single pulse (8 ns) from an ArF excimer laser ( $\lambda=193$  nm, TeoSys LLC, Crofton, MD) volatilized the gelatin on the print ribbon and transferred mESCs from ribbon to receiving substrate (Fig. 1). Motorized, computer-controlled stages for both the receiving substrate and ribbon allowed CAD/CAM-controlled deposition of cells. A CCD camera imaging system coincident with the laser focus allowed real-time observation of cells before and after transfer [45]. After allowing six hours for cell attachment, sufficient maintenance media without LIF was added to cover the cells. Media was changed after 24 hours.

LDW printing parameters were adjusted to control colony size and cell density within colonies. To control the size of a colony, cells were deposited in a precise array, such that a larger printed area, comprised of partially overlapping cell colonies, was achieved (Fig. 2). One colony was printed per cover slip to ensure that printed colonies were independent. This area was treated as a single larger colony, and the colony diameter was measured. In this study, planar arrays were printed with  $1 \times 1$ ,  $2 \times 2$ , and  $3 \times 3$  geometries to generate a distribution of colony sizes (Fig. 2). To adjust cell density in the printed colony, the number of cells on the print ribbon was controlled, and dense or sparse regions of cells on the ribbon

were selected for printing, based on the desired printing density. Cells on the ribbon were visualized in real-time on the print ribbon with a CCD camera, and were selected for transfer by moving the ribbon via a motorized stage. Although some cell scattering occurred immediately after printing, all density classification was performed after any such scattering event. To determine cell density, the area of a representative subset of the colony, the “region of interest”, was measured using Axiovision software on a Zeiss Z1 microscope (Carl Zeiss, Thornwood, NY), and cells within the region were counted with the aid of the Cell Counter Plugin in ImageJ (US National Institutes of Health Bethesda, MD, USA) to mark counted cells. Cell densities within each printed colony were calculated as the number of cells per unit area, and densities were ranked and binned. Printed densities were classified as “low” (cells/cm<sup>2</sup> < 25,000; n=10), “medium” (25,000 cells/cm<sup>2</sup> < 125,000; n=11), or “high” (cells/cm<sup>2</sup> ≥ 125,000; n=11) (Fig. 2). Transferred cells were allowed to grow in maintenance media without LIF until EBs formed, typically after 3–5 days in culture. In this study, EBs were visualized and measured after 3 days in culture.

### 2.3 Image and statistical analysis

Cells were visualized, and the laser-printed colony and EB diameters were measured with Axiovision software on a Zeiss Z1 microscope (Carl Zeiss). Diameters of all EBs near the original printed colony were measured and averaged. If the EB was not circular, the diameter along the longest dimension was measured. Statistical analysis was performed using the software package R (v 3.0.1, The R Project for Statistical Computing, Vienna, Austria). Linear models that colony diameter or cell density within a colony influence EB diameter were constructed. Two-way ANOVAs for these models and their interactions were performed, and post-hoc Tukey’s Honestly Significant Difference tests were used to more closely examine the effect of cell density on EB size.

## 3. Results

### 3.1 Cell growth and EB formation

The motivation for using LDW to control EB size is that the printing technique enables precise placement of EBs and, as a result, additional control over the stem cell microenvironment compared to methods that can be used to manipulate EB size, but not placement. LDW was used to print colonies of mESCs, with independent control of colony size and cell density within the printed colony (Fig. 3). After printing with LDW, cell growth and proliferation were observed, and aggregates close to the original pattern were visible at 24 hours. While some cell scattering was occasionally observed immediately after printing, once the cells attached to the substrate, they remained localized. EBs formed on the glass substrates within a few days with visible 3D growth (Fig. 4). We observed that the entire EB is not in the same focal plane, and EB centers appear darker than the edges in phase contrast microscopy, indicating a 3D cellular structure due to EB formation. Multiple EBs formed within colonies, and the cell distribution within each colony was relatively uniform after printing. As a result, little to no agglomeration was apparent. At high printing densities, EBs formed with diameters greater than 200 μm, with some EB diameters more than 300 μm. However, at low and medium densities, it appeared that smaller EBs formed, with many with diameters smaller than 100 μm. A small number of EBs lifted from the

substrate, but most maintained registry to the original printed pattern; the geometry and size of the pattern was preserved over multiple days.

### 3.2 Influence of printing parameters on EB size

To test the hypotheses that colony size and cell density each influences EB diameter, mESCs were deposited via LDW at different initial colony sizes and densities. EB diameters were measured three days after printing. The EB diameter did not appear to depend on the colony diameter ( $p = 0.74$ ), and a scatter plot of EB diameter against colony diameter did not show an apparent trend (Fig. 5,  $R^2 = 0.004$ ). However, printing density had a significant influence on EB diameter ( $p = 0.0002$ ), and box plots of EB diameter against colony density show disparate EB size when cell density within colonies is adjusted (Fig. 6). There was no significant interaction between colony diameter and cell density within colonies ( $p = 0.44$ ), further indicating the importance of cell density.

Post-hoc analysis with Tukey's Honestly Significant Difference Test showed a significant difference in EB size when cell colonies were printed at high density vs. low density ( $p=0.0005$ ) and high density vs. medium density ( $p = 0.002$ ). However, there was no difference in EB size when colonies were printed at low or medium densities ( $p = 0.83$ ). Using this model to predict EB size, low and medium printing densities will yield EBs with approximately 100- $\mu\text{m}$  diameters, while a high printing density will yield EBs with 170- $\mu\text{m}$  diameters.

## 4. Discussion

We have shown that we can influence the size of the EB formed by mESCs on a homogeneous substrate by controlling the initial cell density through LDW printing, and EB size is independent of the colony size. It has been previously shown that both EB and colony size influence ESC differentiation [13,20,21]. The fact that EB size is influenced by the density of printed cells, but not by the printed colony size, highlights the importance of LDW for creating well-defined stem cell microenvironments to understand and direct stem cell differentiation. For example, colony size and EB size can be controlled independently by LDW and optimized to direct cell differentiation to a desired fate, which is unachievable using conventional approaches. Moreover, LDW allows cell colonies to be placed at controlled distances from one another, enabling paracrine signaling to be modulated as another factor that may influence differentiation. The spatial precision offered by LDW provides a high degree of control for applications in tissue engineering and construct fabrication using a variety of biomaterials and cell types [46–49]. The possible complex configurations afforded by LDW allows many aspects of the stem cell niche to be replicated *in vitro*, and will enable better guidance of stem cell fate decisions.

Unrestricted growth potential after EB formation on the same substrate is important for proliferation of differentiated cells and generation of a suitable cell population. Cell growth is permitted without traumatic events such as trypsinization or cell scraping during the differentiation process. Sequential differentiation on a single substrate will allow streamlined processing and better defined growth environments beginning with the initial printed pattern. Methods that generate EBs in isolation or stirred suspension eliminate the

defined control of cellular location. Using our method, initial cell location is controlled by printing, and subsequent cellular location is defined only by cell proliferation and outgrowth, not by removal and reseeded of cells. Cell migration on the substrate is not restricted, therefore some minor heterogeneities in cell density may develop within a colony. This unrestricted growth enables EB formation. We have shown control of EB size based on printing density, even though cells are free to migrate from the initial printed colony. This level of control may allow for more reproducible differentiation *in vitro*. Although it has been suggested that static suspension culture produces inefficient differentiation because of EB agglomeration [5,29], our method of printing cells yields EBs of controlled size. Previous studies with static suspension culture were unable to control random cell settling on a surface, which may have led to disparate cellular aggregation and uncontrolled EB formation. Our method may improve the differentiation efficiency of static suspension culture, and it offers levels of control unrealized in many other differentiation experiments.

EB formation directly on the substrate typically does not produce EBs of high differentiation potential because of aggregation of EBs in high-density culture, or agglomeration [50,51]. EB size is typically difficult to control in this manner using traditional methods, because when ESCs are randomly seeded, they aggregate based on the cells in their immediate proximity. With random seeding, the number of cells in proximity with a given cell is not well controlled. LDW enables much more rigorous control over spatial patterning and local cell density. Moreover, global density on the substrate can also be rigorously controlled by adjusting the number and location of printed spots. Alternative methods for controlling local cell density involve modifying the substrate, either by creating wells [15,34] or patterning adhesive proteins [19,20]. Agglomeration may be more likely when EBs are randomly dispersed, but printing by LDW enables EB formation in controlled, localized areas. Thus, cellular printing by LDW may have an added benefit for EB differentiation with implications in directing differentiation for tissue engineering applications.

The importance of controlled EB formation in regulating stem cell fate decisions has been documented through studies using micropatterned surfaces or wells [28], including enhanced self-renewal [34,52,53], directed cardiogenesis or endothelial cell differentiation [14,23,54], increased hepatic and cardiac cells [55], and induced cardiomyocytes [22,56]. In general, the growth and differentiation potential of EBs generated in these microwells are limited by the size of the wells and number of cells loaded in each well. 1000-cell EBs have demonstrated superior performance [15] and are generally chosen as the starting cell number for EB formation by hanging drops [57] or microwell chips [55]. However, the EB size is usually 200  $\mu\text{m}$  or larger, which is inherently associated with limited mass transfer and potentially inefficient differentiation [37]. Based on the results herein, printing colonies with cell densities lower than 125,000 cells/ $\text{cm}^2$  enables reliable generation of sub-200- $\mu\text{m}$ -diameter EBs, even down to 100  $\mu\text{m}$ . In this work, the range of cell number per colony was 20 to 10000 (extrapolated by cell density  $\times$  colony diameter), so a large range of cell numbers can be selected. It may not be feasible to simultaneously control cell placement in a desired colony size and at a desired density with conventional methods. The cell placement capabilities offered by LDW allow both size-controlled EBs via printed cell density and minimized agglomeration because cell settling is not random.

While LDW offers precision for controlling local cell density and spacing, there may be some limitations to utilizing this technique in applications with different properties, such as alternate substrates or cell types. This study was performed with CCE mESCs, and other ESC cell lines may have different attachment properties to other cells or the substrate. Moreover, the use of alternate substrates may change the cell-substrate attachment due to the presence or absence of different surface moieties [58]. Cells with poorer substrate attachment capabilities may scatter more after printing, resulting in a lower cell density, and concomitant lower EB size. Additionally, some media formulations inhibit 3D growth and EB formation, so EB generation in static conditions may be limited to specific cell types. Nevertheless, LDW can be utilized to control cell density and colony size and, thus, may prove highly useful in manipulating stem cell microenvironments, provided the cells are adherent. The results herein were obtained on glass cover slips, and EB size can be further tuned based on the hydrophilicity of the substrate [59] and components in the media. While we did not generate single EBs from a printed colony, it may be possible to do so with a sufficiently small colony and a high enough density. In our smaller colonies (300- $\mu\text{m}$ -diameter) with high cell density, we observed formation of as few as three EBs. Thus, we believe that generation of single EB-forming colonies may be achievable with a smaller laser beam spot size. However, single EBs may require geometric constraints on cell migration.

High-density colonies formed significantly larger EBs, suggesting that printed mESCs quickly aggregate with nearby cells. Control of size and EB localization will be further improved by minimizing cell scatter on the substrate immediately after printing. While the effect on differentiation remains to be shown, EBs can be engineered to a desired size by controlling printing density, which will influence design of future differentiation studies. Using LDW, engineered EBs can be printed on homogeneous substrates with unrestricted growth and interactions. After the initial microenvironment is created, cells can proliferate and differentiate, potentially without the need for enzymatic or mechanical treatment. The ability to manipulate printing density, colony size, EB size, and the printed substrate via LDW will enable us to better understand and direct *in vitro* differentiation.

## Conclusions

LDW can be used as a tool to engineer stem cell microenvironments with precise control over cell-cell interactions. Various cellular interaction parameters, including size of the cell colony and EB size, have been shown to influence stem cell differentiation. It is of paramount importance to control these aspects of stem cell interactions independently to improve our ability to direct stem cell differentiation. In this study, we show that using LDW to control the local cell density of patterned stem cells, using mESCs as a model system, is a novel way to directly influence the diameter of the EBs that form. The LDW approach can also be used to control the diameter of the stem cell colony, or in other words, the physical footprint of the printed area. We found that the EB diameter is solely determined by the cell printing density and is independent of the size of the printed colony. Therefore, we provide a new avenue to understand and direct stem cell fate decisions by precisely manipulating EB size and colony size independently or in combination. Control



over both EB size and colony area makes LDW a powerful tool to study cellular interactions and their effects on stem cell differentiation.

## Acknowledgments

This work was supported by NIH R56-DK088217 (DTC/YX) and FA9550-11-C-0028 awarded by DoD, Air Force Office of Scientific Research, National Defense Science and Engineering Graduate (NDSEG) Fellowship, 32 CFR 168a (ADD).

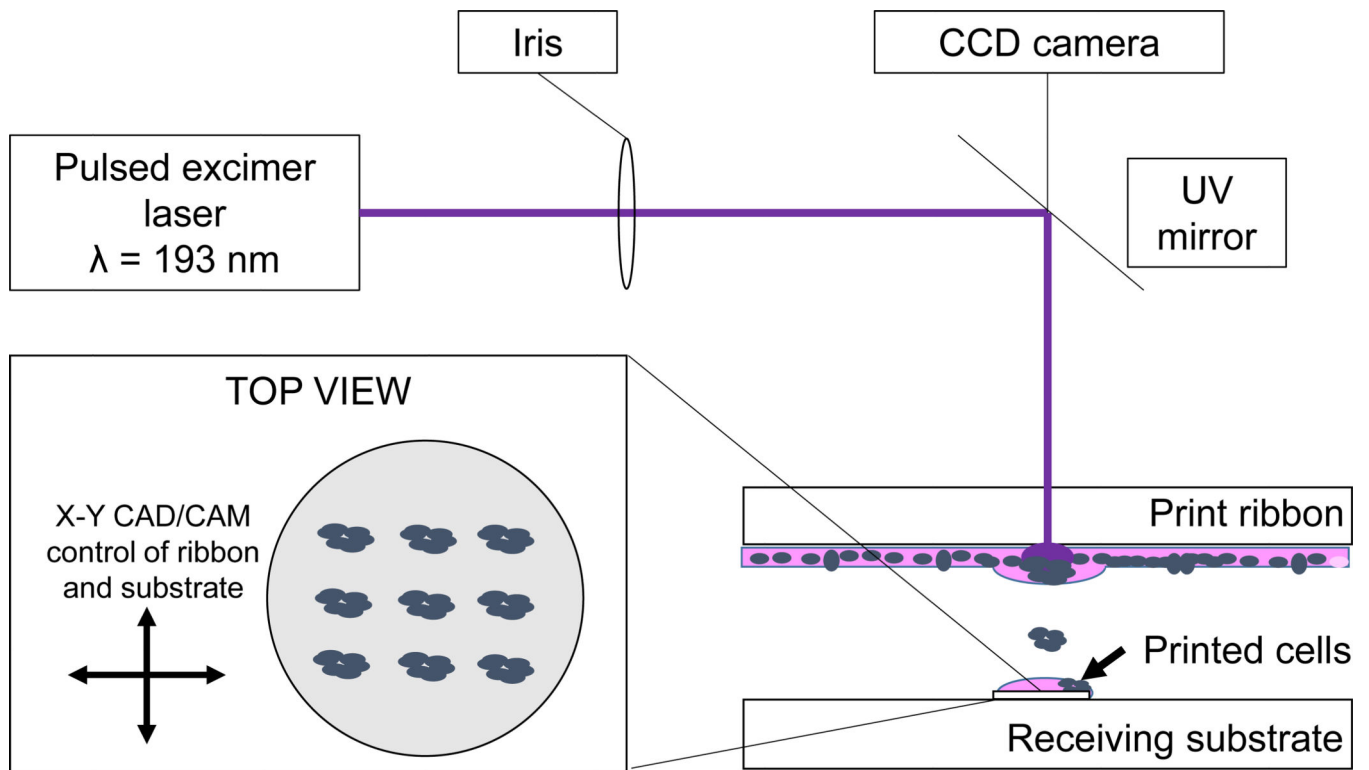
## References

1. Keller G. Embryonic stem cell differentiation: emergence of a new era in biology and medicine. *Genes & development*. 2005; 19:1129–1155. [PubMed: 15905405]
2. Lee AS, Tang C, Rao MS, Weissman IL, Wu JC. Tumorigenicity as a clinical hurdle for pluripotent stem cell therapies. *Nature Medicine*. 2013; 19:998–1004.
3. Murry CE, Keller G. Differentiation of embryonic stem cells to clinically relevant populations: lessons from embryonic development. *Cell*. 2008; 132:661–680. [PubMed: 18295582]
4. Sverdlov ED, Mineev K. Mutation rate in stem cells: an underestimated barrier on the way to therapy. *Trends in molecular medicine*. 2013; 19:273–280. [PubMed: 23481596]
5. Bratt-Leal AM, Carpenedo RL, McDevitt TC. Engineering the embryoid body microenvironment to direct embryonic stem cell differentiation. *Biotechnology Progress*. 2009; 25:43–51. [PubMed: 19198003]
6. Leahy, a; Xiong, JW.; Kuhnert, F.; Stuhlmann, H. Use of developmental marker genes to define temporal and spatial patterns of differentiation during embryoid body formation. *The Journal of Experimental Zoology*. 1999; 284:67–81. [PubMed: 10368935]
7. Carpenedo RL, Bratt-Leal AM, Marklein Ra, Seaman Sa, Bowen NJ, McDonald JF, McDevitt TC. Homogeneous and organized differentiation within embryoid bodies induced by microsphere-mediated delivery of small molecules. *Biomaterials*. 2009; 30:2507–2515. [PubMed: 19162317]
8. Guilak F, Cohen DM, Estes BT, Gimble JM, Liedtke W, Chen CS. Control of stem cell fate by physical interactions with the extracellular matrix. *Cell Stem Cell*. 2009; 5:17–26. [PubMed: 19570510]
9. Sun Y, Villa-Diaz LG, Lam RHW, Chen W, Krebsbach PH, Fu J. Mechanics regulates fate decisions of human embryonic stem cells. *PloS one*. 2012; 7:e37178. [PubMed: 22615930]
10. Mochizuki H, Ohnuki Y, Kurosawa H. Effect of glucose concentration during embryoid body (EB) formation from mouse embryonic stem cells on EB growth and cell differentiation. *JBIOSC*. 2011; 111:92–97.
11. Tonge PD, Olariu V, Coca D, Kadirkamanathan V, Burrell KE, Billings SA, Andrews PW. Prepatterning in the stem cell compartment. *PLoS One*. 2010; 5:e10901. [PubMed: 20531938]
12. Talavera-Adame D, Gupta A, Kurtovic S, Chaiboonma KL, Arumugaswami V, Dafoe DC. BMP-2/-4 Upregulation Promoted by Endothelial Cells in Co-Culture Enhances Mouse Embryoid Body Differentiation. *Stem Cells and Development*. 2013 **Epub ahead**.
13. Bauwens CL, Peerani R, Niebruegge S, Woodhouse KA, Kumacheva E, Husain M, Zandstra PW. Control of human embryonic stem cell colony and aggregate size heterogeneity influences differentiation trajectories. *Stem Cells*. 2008; 26:2300–2310. [PubMed: 18583540]
14. Bauwens CL, Song H, Thavandiran N, Ungrin M, Masse S, Nanthakumar K, Seguin C, Zandstra PW. Geometric control of cardiomyogenic induction in human pluripotent stem cells. *Tissue Engineering: Part A*. 2011; 17:1901–1909. [PubMed: 21417693]
15. Yanai A, Laver CR, Joe AW, Viringipurampeer IA, Wang X, Gregory-Evans CY, Gregory-Evans K. Differentiation of human embryonic stem cells using size-controlled embryoid bodies and negative cell selection in the production of photoreceptor precursor cells. *Tissue Engineering Part C: Methods*. 2013 **Epub ahead**.
16. Carpenedo RL, Seaman SA, McDevitt TC. Microsphere size effects on embryoid body incorporation and embryonic stem cell differentiation. *Journal of Biomedical Materials Research Part A*. 2010; 94:466–475. [PubMed: 20213812]

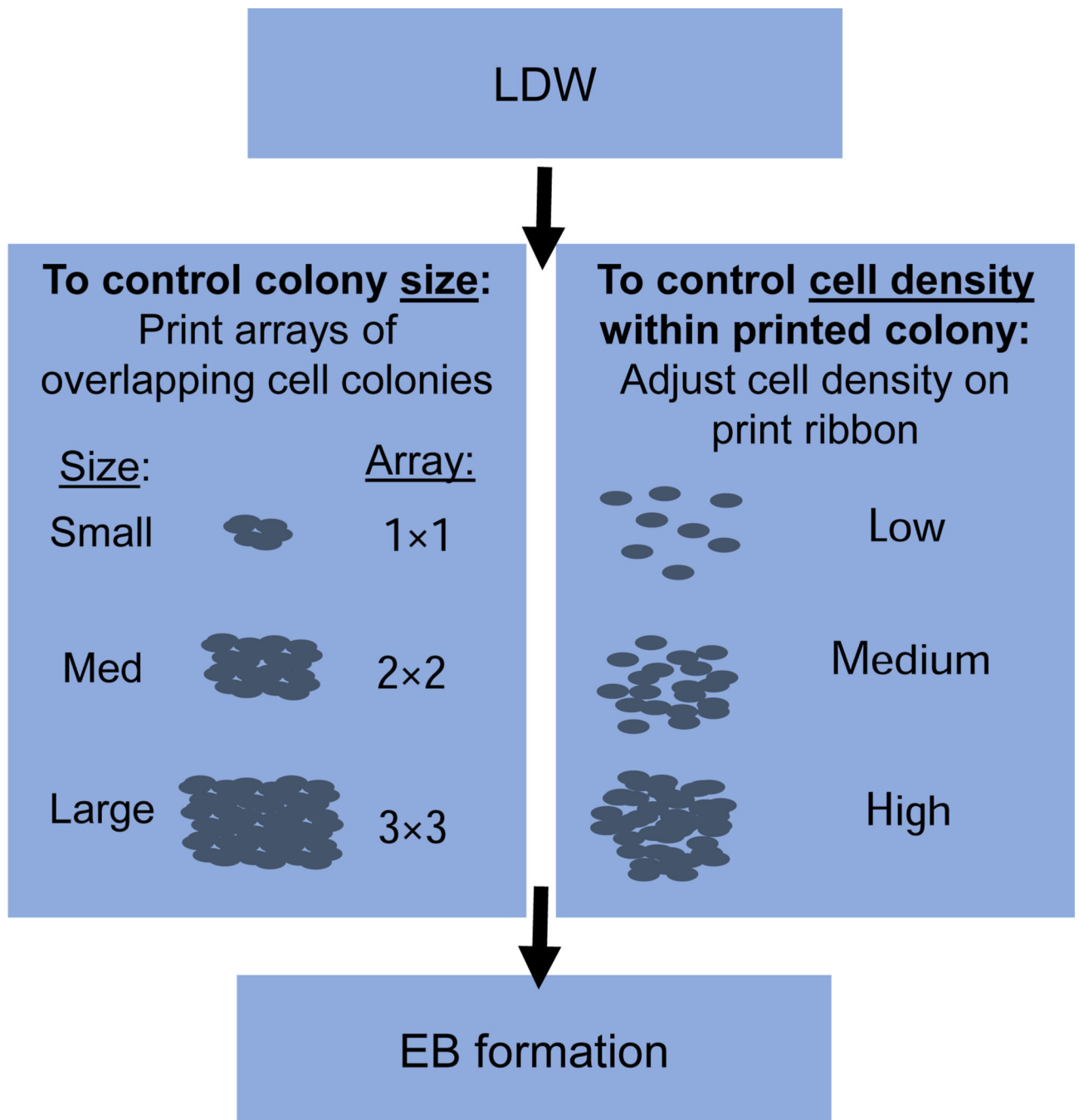
17. Messana JM, Hwang NS, Coburn J, Elisseeff JH, Zhang Z. Size of the embryoid body influences chondrogenesis of mouse embryonic stem cells. *Journal of Tissue Engineering and Regenerative Medicine*. 2008; 2:499–506. [PubMed: 18956411]
18. Sasaki D, Shimizu T, Masuda S, Kobayashi J, Itoga K, Tsuda Y, Yamashita JK, Yamato M, Okano T. Mass preparation of size-controlled mouse embryonic stem cell aggregates and induction of cardiac differentiation by cell patterning method. *Biomaterials*. 2009; 30:4384–4389. [PubMed: 19487020]
19. Park J, Cho C, Parashurama N, Li Y, Berthiaume F, Toner M, Tilles AW, Yarmush ML. Microfabrication-based modulation of embryonic stem cell differentiation. *Lab Chip*. 2007; 7:1018–1028. [PubMed: 17653344]
20. Lee LH, Peerani R, Ungrin M, Joshi C, Kumacheva E, Zandstra PW. Micropatterning of human embryonic stem cells dissects the mesoderm and endoderm lineages. *Stem Cell Research*. 2009; 2:155–162. [PubMed: 19383420]
21. Peerani R, Rao BM, Bauwens C, Yin T, Wood GA, Nagy A, Kumacheva E, Zandstra PW. Niche-mediated control of human embryonic stem cell self-renewal and differentiation. *The EMBO journal*. 2007; 26:4744–4755. [PubMed: 17948051]
22. Choi YY, Chung BG, Lee DH, Khademhosseini A, Kim J-H, Lee S-H. Controlled-size embryoid body formation in concave microwell arrays. *Biomaterials*. 2010; 31:4296–4303. [PubMed: 20206991]
23. Hwang Y-S, Chung BG, Ortmann D, Hattori N, Moeller H-C, Khademhosseini A. Microwell-mediated control of embryoid body size regulates embryonic stem cell fate via differential expression of WNT5a and WNT11. *Proceedings of the National Academy of Sciences of the United States of America*. 2009; 106:16978–16983. [PubMed: 19805103]
24. Desbaillets I, Ziegler U, Groscurth P, Gassmann M. Embryoid bodies: an in vitro model of mouse embryogenesis. *Experimental Physiology*. 2000; 85:645–651. [PubMed: 11187960]
25. Faulkner-Jones A, Greenhough S, A King J, Gardner J, Courtney A, Shu W. Development of a valve-based cell printer for the formation of human embryonic stem cell spheroid aggregates. *Biofabrication*. 2013; 5:015013. [PubMed: 23380571]
26. Xu F, Sridharan B, Wang S, Gurkan UA, Syverud B, Demirci U. Embryonic stem cell bioprinting for uniform and controlled size embryoid body formation. *Biomicrofluidics*. 2011; 5:22207. [PubMed: 21799713]
27. Kim C, Lee IH, Lee K, Ryu SS, Lee SH, Lee K, Lee JL, Kang JY, Kim TS. Multi-Well Chip for Forming a Uniform Embryoid Body in a Tiny Droplet with Mouse Embryonic Stem Cells. *Biosci. Biotechnol. Biochem*. 2007; 71:2985–2991. [PubMed: 18071258]
28. Kurosawa H. Methods for inducing embryoid body formation: in vitro differentiation system of embryonic stem cells. *Journal of Bioscience and Bioengineering*. 2007; 103:389–398. [PubMed: 17609152]
29. Carpenedo RL, Sargent CY, McDevitt TC. Rotary suspension culture enhances the efficiency, yield, and homogeneity of embryoid body differentiation. *Stem Cells*. 2007; 25:2224–2234. [PubMed: 17585171]
30. Hunt MM, Meng G, Rancourt DE, Gates ID, Kallos MS. Factorial Experimental Design for the Culture of Human Embryonic Stem Cells as Aggregates in Stirred Suspension Bioreactors Reveals the Potential for Interaction Effects Between Bioprocess Parameters. *Tissue Engineering: Part C*. 2013; 20:1–36.
31. Valamehr B, Jonas S, Polleux J. Hydrophobic surfaces for enhanced differentiation of embryonic stem cell-derived embryoid bodies. *Proceedings of the National Academy of Sciences*. 2008; 105:14459–14464.
32. Ng ES, Davis RP, Azzola L, Stanley EG, Elefanty AG. Forced aggregation of defined numbers of human embryonic stem cells into embryoid bodies fosters robust, reproducible hematopoietic differentiation. *Blood*. 2005; 106:1601–1603. [PubMed: 15914555]
33. Giobbe GG, Zagallo M, Riello M, Serena E, Masi G, Barzon L, Di Camillo B, Elvassore N. Confined 3D microenvironment regulates early differentiation in human pluripotent stem cells. *Biotechnology and Bioengineering*. 2012; 109:3119–3132. [PubMed: 22674472]

34. Mohr JC, de Pablo JJ, Palecek SP. 3-D microwell culture of human embryonic stem cells. *Biomaterials*. 2006; 27:6032–6042. [PubMed: 16884768]
35. Ungrin MD, Joshi C, Nica A, Bauwens C, Zandstra PW. Reproducible, ultra high-throughput formation of multicellular organization from single cell suspension-derived human embryonic stem cell aggregates. *PLoS ONE*. 2008; 3:e1565. [PubMed: 18270562]
36. Zhang Y, Xia Y. Formation of Embryoid Bodies with Controlled Sizes and Maintained Pluripotency in Three-Dimensional Inverse Opal Scaffolds. *Advanced Functional Materials*. 2012; 22:121–129.
37. Van Winkle AP, Gates ID, Kallos MS. Mass transfer limitations in embryoid bodies during human embryonic stem cell differentiation. *Cells Tissues Organs*. 2012; 196:34–47. [PubMed: 22249133]
38. Earls JK, Jin S, Ye K. Mechanobiology of human pluripotent stem cells. *Tissue Engineering: Part B*. 2013; 19:420–430.
39. Kim JM, Moon S-H, Lee SG, Cho YJ, Hong KS, Lee JH, Lee HJ, Chung H-M. Assessment of differentiation aspects by the morphological classification of embryoid bodies derived from human embryonic stem cells. *Stem cells and development*. 2011; 20:1925–1935. [PubMed: 21388292]
40. Raof NA, Schiele NR, Xie Y, Chrisey DB, Corr DT. The maintenance of pluripotency following laser direct-write of mouse embryonic stem cells. *Biomaterials*. 2011; 32:1802–1808. [PubMed: 21168910]
41. Robertson E, Bradley A, Kuehn M, Evans M. Germ-line transmission of genes introduced into cultured pluripotential cells by retroviral vector. *Nature*. 1986; 323:445–448. [PubMed: 3762693]
42. Keller G, Kennedy M, Papayannopoulou T, Wiles MV. Hematopoietic commitment during embryonic stem cell differentiation in culture. *Molecular and Cellular Biology*. 1993; 13:473–486. [PubMed: 8417345]
43. Schiele NR, Chrisey DB, Corr DT. Gelatin-based laser direct-write technique for the precise spatial patterning of cells. *Tissue Engineering Part C: Methods*. 2011; 17:289–298. [PubMed: 20849381]
44. Dias, AD.; Schiele, NR.; Carr, BM.; Raof, NA.; Xie, Y.; Chrisey, DB.; Corr, DT. Using Laser Direct-Write to Precisely Pattern Cells on Glass Cover Slips; Proceedings of the IEEE 37th Annual Northeast Bioengineering Conference (NEBEC); 2011.
45. Schiele NR, Koppes RA, Corr DT, Ellison KS, Thompson DM, Ligon LA, Lippert TKM, Chrisey DB. Laser direct writing of combinatorial libraries of idealized cellular constructs: Biomedical applications. *Applied Surface Science*. 2009; 255:5444–5447.
46. Schiele NR, Corr DT, Huang Y, Raof NA, Xie Y, Chrisey DB. Laser-based direct-write techniques for cell printing. *Biofabrication*. 2010; 2:032001. [PubMed: 20814088]
47. Riggs BC, Dias AD, Schiele NR, Cristescu R, Huang Y, Corr DT, Chrisey DB. Matrix-assisted pulsed laser methods for biofabrication. *MRS Bulletin*. 2011; 36:1043–1050.
48. Ovsianikov A, Gruene M, Pflaum M, Koch L, Maiorana F, Wilhelm M, Haverich A, Chichkov B. Laser printing of cells into 3D scaffolds. *Biofabrication*. 2010; 2:014104. [PubMed: 20811119]
49. Gruene M, Deiwick A, Koch L, Schlie S, Unger C, Hofmann N, Bernemann I, Glasmacher B, Chichkov B. Laser printing of stem cells for biofabrication of scaffold-free autologous grafts. *Tissue Engineering Part C: Methods*. 2011; 17:1–36.
50. Dang S, Kyba M, Perlingeiro R. Efficiency of embryoid body formation and hematopoietic development from embryonic stem cells in different culture systems. *Biotechnology and Bioengineering*. 2002; 78:442. [PubMed: 11948451]
51. Dang SM, Gerecht-Nir S, Chen J, Itskovitz-Eldor J, Zandstra PW. Controlled, scalable embryonic stem cell differentiation culture. *Stem Cells*. 2004; 22:275–282. [PubMed: 15153605]
52. Khademhosseini A, Ferreira L, Blumling J, Yeh J, Karp JM, Fukuda J, Langer R. Co-culture of human embryonic stem cells with murine embryonic fibroblasts on microwell-patterned substrates. *Biomaterials*. 2006; 27:5968–5977. [PubMed: 16901537]
53. Sakai Y, Yoshiura Y, Nakazawa K. Embryoid body culture of mouse embryonic stem cells using microwell and micropatterned chips. *Journal of Bioscience and Bioengineering*. 2011; 111:85–91. [PubMed: 20863754]
54. Schukur L, Zorlutuna P, Cha JM, Bae H, Khademhosseini A. Directed differentiation of size-controlled embryoid bodies towards endothelial and cardiac lineages in RGD-modified

- poly(ethylene glycol) hydrogels. *Advanced Healthcare Materials*. 2013; 2:195–205. [PubMed: 23193099]
55. Nakazawa K, Yoshiura Y, Koga H, Sakai Y. Characterization of mouse embryoid bodies cultured on microwell chips with different well sizes. *Journal of Bioscience and Bioengineering*. 2013 **In press**.
  56. Mohr J, Zhang J, Azarin S, Soerens A, de Pablo JJ, Thomson JA, Lyons GE, Palacek SP, Kamp TJ. The microwell control of embryoid body size in order to regulate cardiac differentiation of human embryonic stem cells. *Biomaterials*. 2010; 31:1–18. [PubMed: 19788947]
  57. Kang X, Xie Y, Powell HM, Lee JL, Belury MA, Lannutti JJ, Kniss DA. Adipogenesis of murine embryonic stem cells in a three-dimensional culture system using electrospun polymer scaffolds. *Biomaterials*. 2007; 28:450–458. [PubMed: 16997371]
  58. Yang J, Mei Y, Hook AL, Taylor M, Urquhart AJ, Bogatyrev SR, Langer R, Anderson DG, Davies MC, Alexander MR. Polymer surface functionalities that control human embryoid body cell adhesion revealed by high throughput surface characterization of combinatorial material microarrays. *Biomaterials*. 2010; 31:8827–8838. [PubMed: 20832108]
  59. Konno T, Akita K, Kurita K, Ito Y. Formation of embryoid bodies by mouse embryonic stem cells on plastic surfaces. *Journal of Bioscience and Bioengineering*. 2005; 100:88–93. [PubMed: 16233856]
  60. Dias, AD.; Xie, Y.; Chrisey, DB.; Corr, DT. Using laser direct-write to influence embryoid body size on uniform substrates. *Proceedings of the ASME Summer Bioengineering Conference; SBC2012–80612*; 2012.

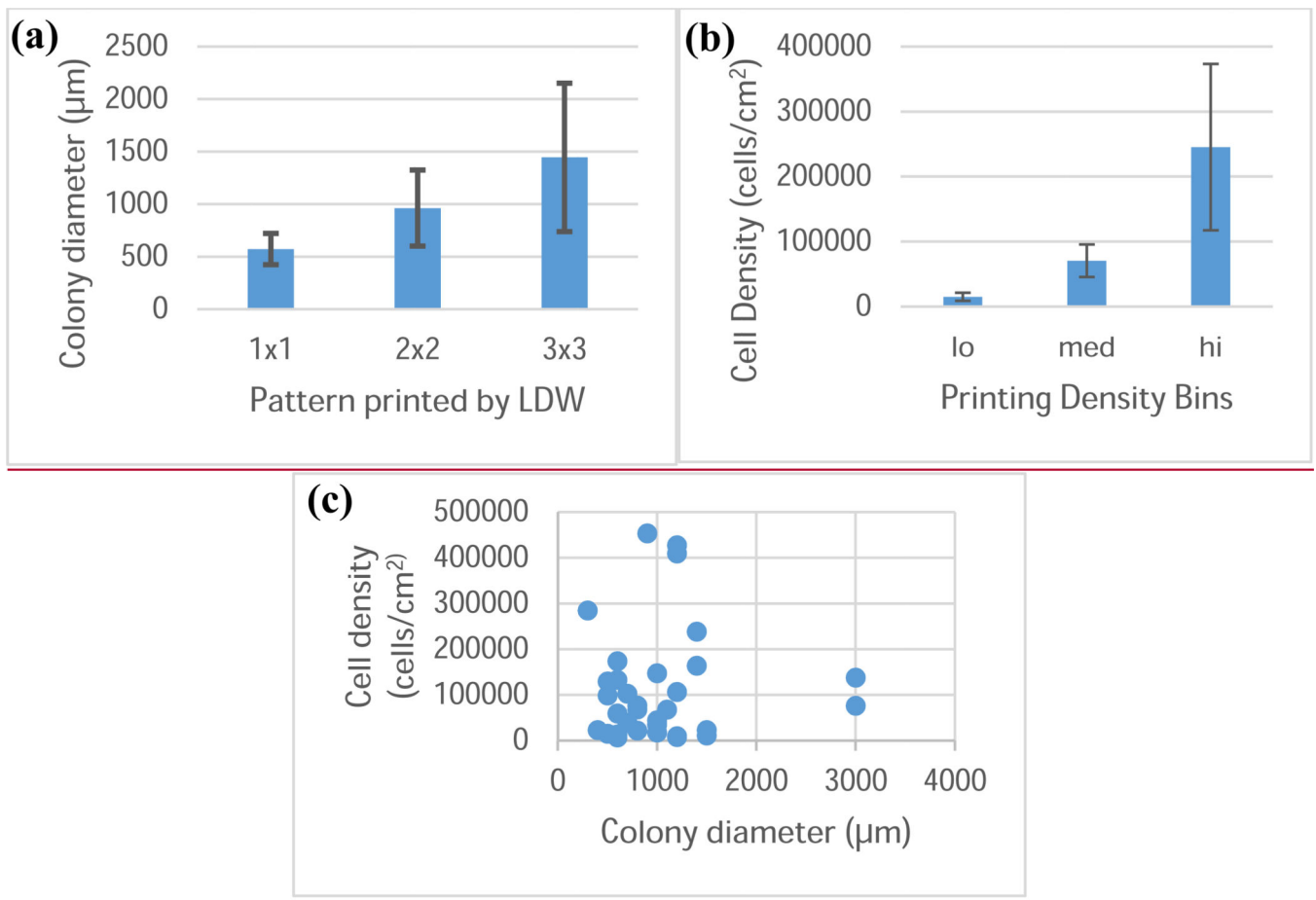


**Figure 1.** LDW schematic for mESC deposition on glass cover slips. Inset – top view of example printed cell configuration.



**Figure 2.**

Schematic for control of colony diameter and cell density within colonies via LDW, and resultant EBs. *Left panel:* colony diameter was controlled by printing arrays of overlapping smaller colonies to generate larger colonies. *Right panel:* cell density within the printed colony was controlled by adjusting the density of cells on the print ribbon. Cell scattering on the substrate also influenced cell density. EB formation from printed patterns was observed and measured after three days in culture.

**Figure 3.**

Control of colony diameter and cell density using LDW. (a) Plot of mESC colony diameter against the pattern printed by LDW. The diameter of the printed colony is controlled by LDW printing parameters, independent of the printing density (error bars:  $\pm 1$  standard deviation). (b) Plot of mESC density in printed colonies, and the binning for analysis. Bins were “low” (cells/ $\text{cm}^2 < 25,000$ ;  $n=10$ ), “medium” ( $25,000 \leq \text{cells}/\text{cm}^2 < 125,000$ ;  $n=11$ ), or “high” ( $\text{cells}/\text{cm}^2 \geq 125,000$ ;  $n=11$ ) density (error bars:  $\pm 1$  standard deviation). (c) Plot of the cell density within a colony against the colony diameter for experiments in this study. These factors can be controlled independently.

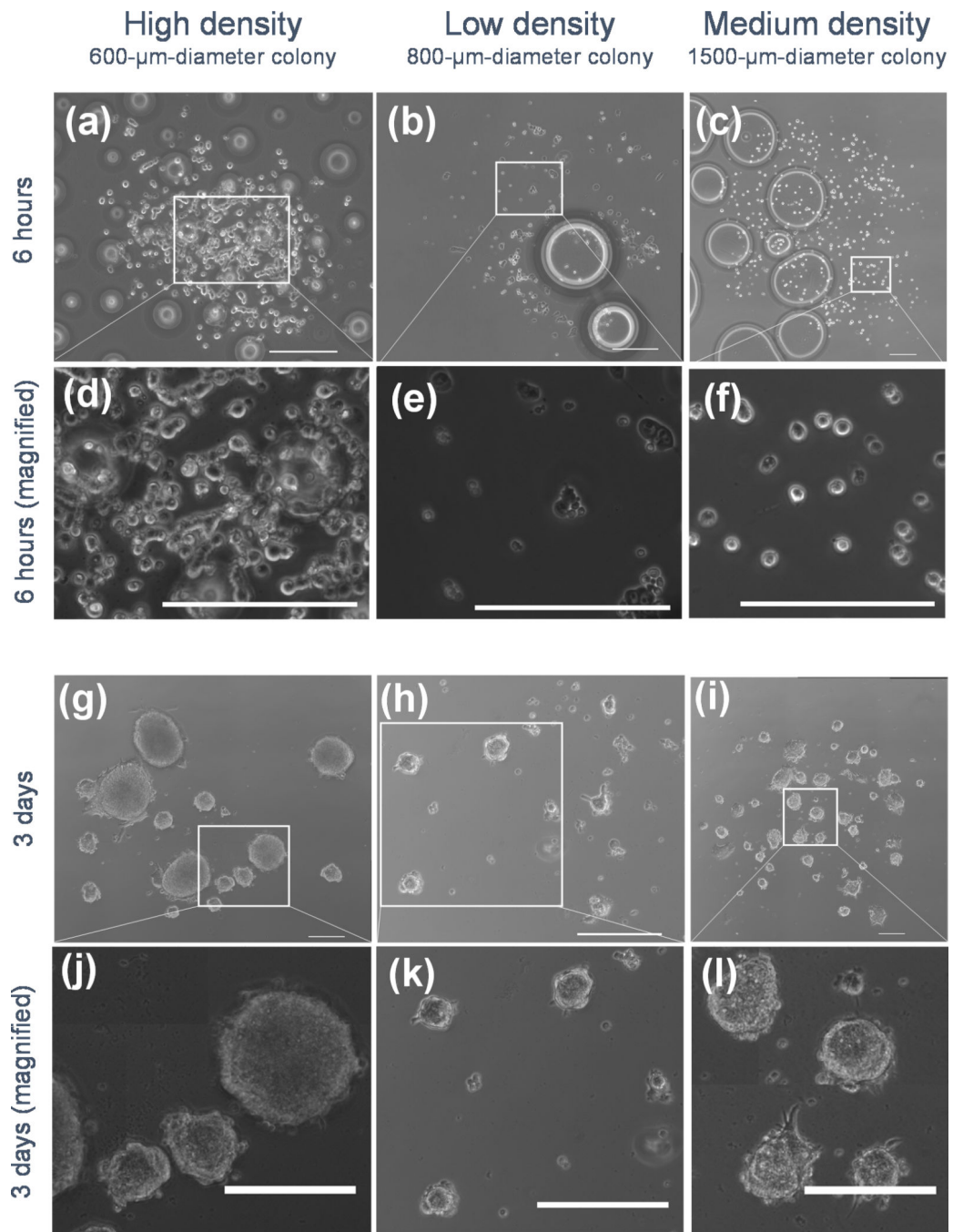


**Figure 4.**

Representative phase contrast images of mESCs after printing (6 hours, a–f) and EB formation (3 days, g–l) from laser direct-written cells. To illustrate that printing density and colony diameter are independent, representative images of multiple initial densities and colony sizes were selected. Initial colony diameters were (a) 600  $\mu\text{m}$  at high density, (b) 800  $\mu\text{m}$  at low density, and (c) 1500  $\mu\text{m}$  at medium density. Magnified images are shown (d–f) to show scale more clearly. Bubbles underneath the cover slips disappear after addition of media liquefies the gelatin securing the cover slip to the Petri dish. Tiled mosaics of EBs



illustrate registry to the initial printed pattern (d–f), and EBs from these patterns are magnified (g–i) to more clearly illustrate scale. Scale bars are 200  $\mu\text{m}$  (adapted from [60]).

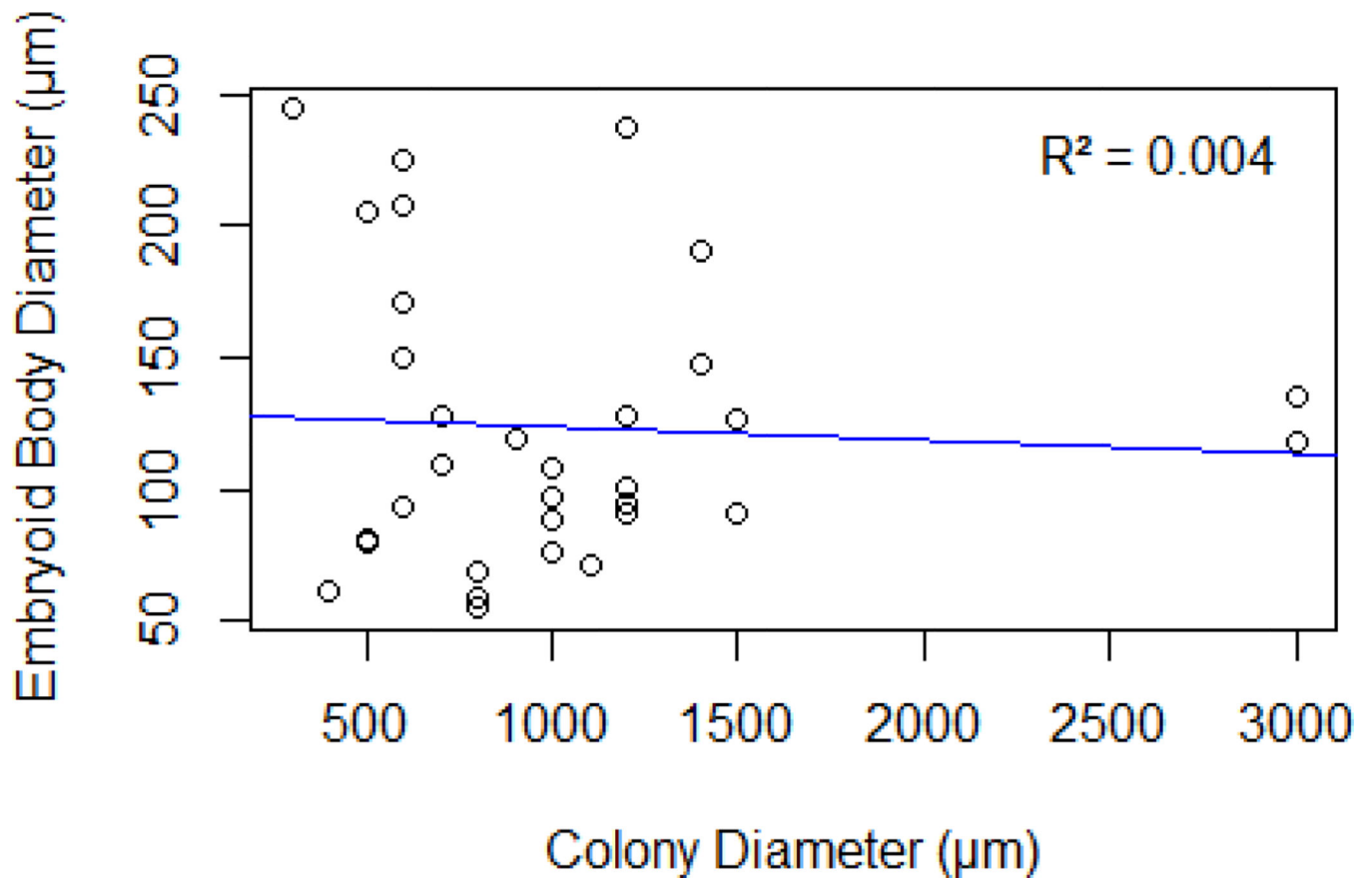


**Figure 5.** EB diameter plotted versus colony diameter, indicating that EB diameter is not correlated ( $R^2 = 0.004$ ) with the diameter of the printed colony (adapted from [60]).

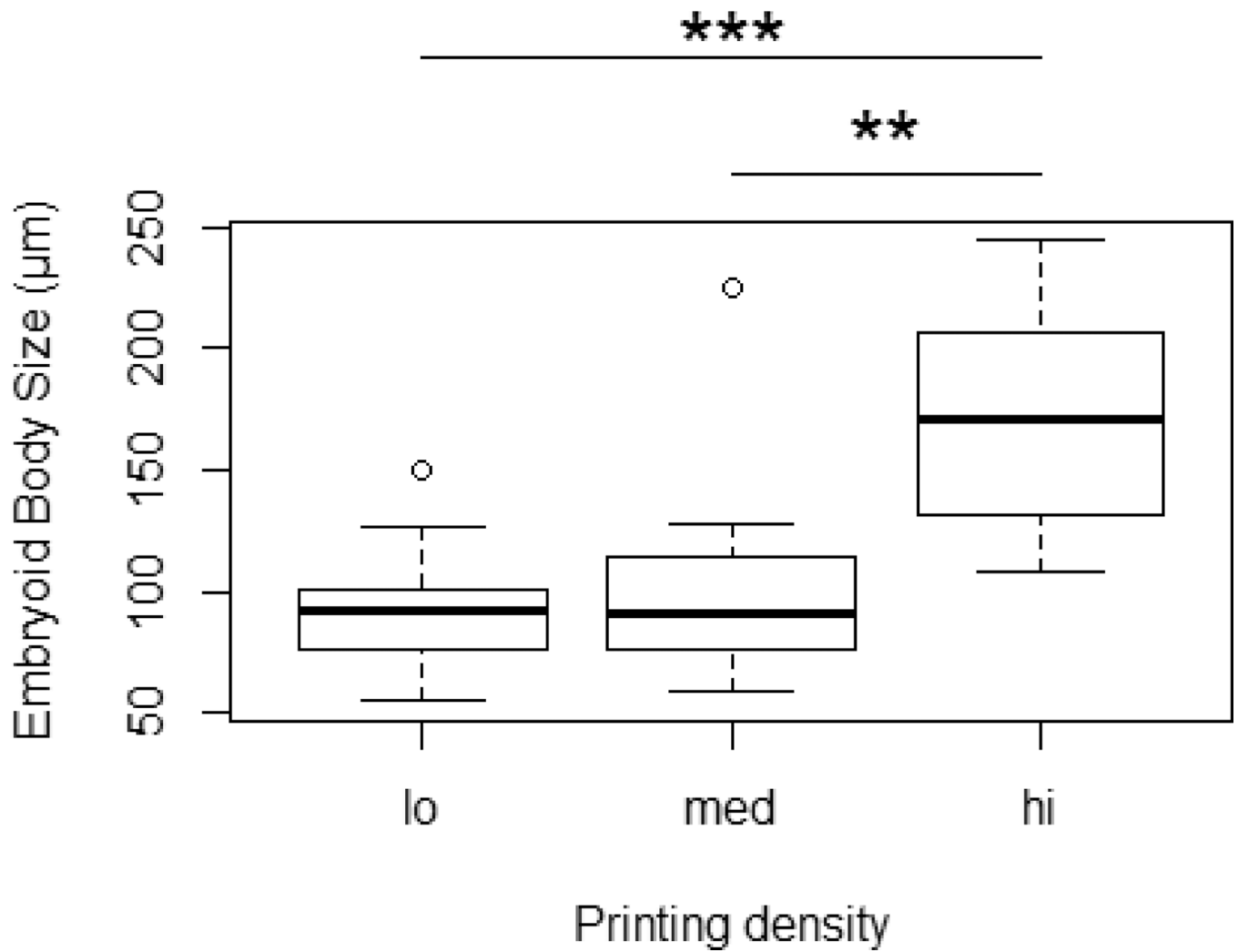


**Figure 6.** Box plot of EB diameter versus printing density showing that EB diameter is significantly increased with a high printed colony density (adapted from [60]).